Three-Dimensional Analysis of Non-Repeatable Runout (NRRO) in Ball Bearings

S. TADA

Non-repeatable runout (NRRO) is one of the characteristics of high precision ball bearings. The decrease of NRRO contributes to the track density improvement (memory capacity improvement) of hard disk drives.

Here, a NRRO analytical program for ball bearings has been developed, and the result of NRRO analysis is shown. The developed program is a 3-dimensional NRRO analytical program which fixes the contact angle, and a static analytical program including the concept of time.

***Key Words**: ball bearing, non-repeatable runout, NRRO, behavior, 3-dimensional analysis*

1. Introduction

One of the indexes that indicate the performance of a ball bearing is Non-repeatable Runout (hereinafter referred to as NRRO). It is one of the important indexes that show a bearing's rotational accuracy. The NRRO of a bearing used for a spindle in a hard disk drive (hereinafter referred to as HDD) is especially important. The NRRO of such a bearing may cause a tracking error that disturbs data reading and writing as well as vibration that may lead to a spindle's resonance, thereby preventing increase in the track density. Thus, in order to reduce NRRO, it is important to find how it is generated within the bearing, and to know the behavior of a rotational ring.

An experimental analysis of NRRO of ball bearings has been dramatically advanced and, especially first-order elements - main NRRO elements of ball bearings - have long been an object of researches and now experimentally clarified through these researchs[1)~6)]. On the other hand, performing the numerical analysis on NRRO in a dynamic manner requires a large amount of calculations. Thus, for the purpose of saving the time needed for such calculations, the following known methods are generally used: 2-dimensional linear analysis method[7)] in which the spring force (elastic resilience) between a ball and raceway is statically linearized in the radial direction (2 degree of freedom); and 2-dimensional non-linear analysis method[8)] that takes into consideration the Hertzian contact on the surface between a ball and raceway. Among these methods, the latter non-linear analysis has proved not only the existence of NRRO's first-order element but also that of the second-order element, details of which, however, have not been clarified. It has been also introduced to use a 2-dimensional non-linear analysis to dynamically analyze two bearings[9)]. Although these conventional methods have achieved the substantial reduction in the calculation time, these achievements have been applied only to the case of NRRO analysis in the radial direction and have not yet been applied to that in the axial direction.

For performing a 3-dimensional NRRO analysis, the use of bearing dynamic analysis software "ADORE"[10)] allows for dynamic analysis of NRRO with 5 degrees of freedom in which the ball contact angle is taken into consideration and non-linear spring characteristic between ball and raceway can be gained by Hertzian contact theory. Using this software provides high precision-analysis in three dimension space regarding the influence on NRRO elements by factors such as the raceway waviness of inner and outer rings, ball pitch error, and the number of balls. The analysis by this software, however, requires a lot of calculation time because this software is a dynamic analysis software that takes into consideration not only a factor of contact condition including lubricant film but also a retainer collision-factor. Furthermore, this software also requires the input of 3-dimensional waviness information for considering the influence by ball waviness that can be analyzed by the above 2-dimensional analysis method, resulting in current situation that the analysis on the ball waviness influence is impossible by this software. Therefore, such a program that can solve the above problems can provide more precise NRRO analysis.

In this paper, the results on the development of a 3-dimensional non-linear NRRO analysis program are described that can take into consideration a ball waviness by using a bearing that has Hertzian contact with a contact angle as an analysis model and by fixing the contact angle (i. e., fixing the bearing revolution axis) and that can substantially reduce the calculation amount by using the concept of time to perform the analysis semi-dynamically.

2. Three-dimensional Analysis of NRRO

2. 1 Analysis Method

NRRO is caused by the wavinesses on the ball surfaces and the inner and outer rings' raceway surfaces, and can be calculated based on the balance of geometric forces. General description on NRRO is omitted in this paper because such a description has been made in many papers and in the last

edition of Koyo Engineering Journal, 160E.

Some publications have already introduced the NRRO programs that take waviness into consideration, in which 0 rad of contact angle is used to provide 2-dimensional analysis program[7), 8)]. This paper, however, describes the method for 3-dimensionally calculating NRRO in which: preload P_L is applied to a bearing with a constant-pressure-preload method that is typically used for measuring NRRO of a single bearing; the contact angle is fixed with an ideal geometric configuration without considering the moment balance; and the balls are equally spaced (i. e., no balls have lead or lag). **Figure 1** shows a schematic diagram of an analysis model whose outer ring is rotating. In **Fig. 1**, the inner ring's geometric center G_i (0, 0, 0) is not changed by the waviness of the raceway and balls' rolling contact surfaces since the inner ring's geometric center is fixed, while outer ring's geometric center G_o (x, y, z) is changed. The balls and inner and outer rings are supported by non-linear springs K_i and K_o respectively, and the contact angle is used when initial preload P_L is applied. This contact angle is in the initial condition and assumed to be constant during the analysis. A rectangular coordinate system as shown in **Fig. 1** was used in which z axis was directed in the axial direction.

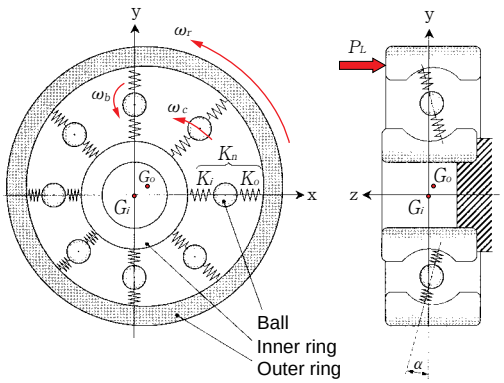

Fig. 1 Schematic of analysis model (outer ring rotation)

Since the wavinesses of ball surface and inner and outer rings' raceways can be developed using Fourier series, it is assumed that: the inner and outer rings' raceway radii are r_i, r_o; ball radius is r_b; the waviness amplitude of each lobe and phase difference therebetween are a_i, a_o, a_b, ϕ_j, respectively. (j: the number of waviness lobes) Then, the waviness configuration functions W_{ij}, W_{oj}, and W_{bj} can be expressed by the following equation (1) at which, after t seconds have passed, the ball contact occurs between the inner and outer rings of the j th ball that has waviness.

$$W_{ij} = r_i + \sum_{k=1}^{N} \{a_{ik} \cos(j\omega_r t - \phi_{ik})\}$$

$$W_{oj} = r_o + \sum_{k=1}^{N} \{a_{ok} \cos(j\omega_c t - \phi_{ok})\}$$

$$W_{bj} = 2r_b + \sum_{k=1}^{N} [a_{bjk}\{\cos(j\omega_b t - \phi_{bjk}) + \cos(j\omega_b t - \phi_{bjk} + \pi)\}] \quad \cdots\cdots (1)$$

Wherein,

ω_c : Ball revolution angular velocity [rad/sec]
ω_b : Ball rotation angular velocity [rad/sec]
ω_r : Outer ring's angular velocity [rad/sec]
i, o, b : Inner ring, outer ring, ball, respectively
j : j th ball
k : Waviness lobe (order)

Based on the above equation (1), the elastic displacement δ_j at the position of j th ball after t seconds have passed can be expressed by the following equation (2).

$$\delta_j = (W_{ij} - W_{oj}) \cos\alpha + W_{bj} + d_{pl} \quad \cdots\cdots (2)$$

wherein, d_{pl}: the elastic deformation in the contact direction with a contact angle α between inner and outer rings and balls which is caused by an initial preload.

According to the Hertzian contact theory, there is the following relation of (3) between a rolling element load Q and an elastic displacement δ in a ball[11)].

$$Q = K_n \delta^{1.5} \quad \cdots\cdots (3)$$

Wherein, K_n is a constant. Assuming the constant between a ball and an inner ring is K_i and that between a ball and an outer ring is K_o, K_n can be expressed by the following equation of (4).

$$K_n = \frac{K_i K_o}{\left(K_i^{2/3} + K_o^{2/3}\right)^{1.5}} \quad \cdots\cdots (4)$$

From the above, assuming that displacements to each axis of outer ring's geometric center are x, y, and z, respectively, the balance of forces among them can be expressed by the following equation of (5).

$$\left.\begin{aligned} &\sum_{j=1}^{Z} K_n\{\delta_j - (x\cos\theta_j + y\sin\theta_j)\cos\alpha - z\sin\alpha\}^{1.5}\cos\alpha\cos\theta_j = 0 \\ &\sum_{j=1}^{Z} K_n\{\delta_j - (x\cos\theta_j + y\sin\theta_j)\cos\alpha - z\sin\alpha\}^{1.5}\cos\alpha\sin\theta_j = 0 \\ &\sum_{j=1}^{Z} K_n\{\delta_j - (x\cos\theta_j + y\sin\theta_j)\cos\alpha - z\sin\alpha\}^{1.5}\sin\alpha = F_a \end{aligned}\right\} \quad \cdots\cdots (5)$$

wherein, θ_j is the angle position of j th ball at any timing (i. e., the angle in the clockwise direction when x axis is assumed to be 0 deg.). The above equation (4) is the balance of the forces in each of x, y, and z directions and by solving this non-linear simultaneous equation, the behavior of the outer ring considering each element's waviness at each timing can be analyzed. It is also assumed that the contact angle α varies depending on a preload but does not vary by the value of waviness and ball rotation axis is fixed. This provides the analysis – although it is partial – of the influence by ball waviness that has been difficult by ADORE. It is noted, however, that the above equations do not take into consideration the change of contact angle due to moment balance, centrifugal force, and waviness.

2. 2 Result of NRRO Analysis Considering Waviness

2. 2. 1 NRRO Considering a Single Waviness

Hereinafter, an example is described in which the equation described in the above chapter is used to prepare a 3-dimensional NRRO analysis program to analyze the relationship between the waviness of balls of inner and outer rings and the outer rings' behavior. Input wavinesses are indicated with total amplitude (p_p value) and NRRO values are indicated by applying the Hanning window to the outer ring's geometric center and then indicating the NRRO value as the amount that is two times the power spectrum value gained by FET analysis (p_p value). It is also assumed that for inner and outer rings' raceway wavinesses, the raceway bottom diameter varies in the radial direction by waviness but the raceway radius (curvature) does not change.

Table 1 shows analysis parameters of a standard model.

Table 2 shows the NRRO frequency appeared for the case where a single waviness is added. In **Table 2**, a waviness element of $nZ\pm1$ lobes also can be confirmed in the linear equation in which the index part of the equation (4) is deleted and the magnitude of NRRO is constant regardless of input parameters such as preload, material, and contact angle. **Figure 2** shows an example of the analysis result. As long as an analysis model is determined, the magnitude of waviness is proportional to that of NRRO elements. However, for balls, increasing the number of balls reduces the magnitude of NRRO (i. e., in a linear model, balls show inversely-proportional characteristic). On the other hand, NRRO elements in the axial direction and elements caused by ball waviness show non-linearity when preload and residual radial clearance (contact angle) change.

Table 1 Standard analysis model

Rotated part	Outer ring	Preload	20N
Preload method	Constant-pressure preload	Young's modulus	2.08×10^{11}Pa
Ball pitch circle diameter	7mm	Poisson's ratio	0.3
Ball diameter	1mm	Radial clearance	10μm
Number of balls	8		

Table 2 NRRO first-order element (single waviness)

Input waviness	Number of waviness lobes	x and y directions [Hz]	z direction [Hz]
Inner ring (stationary)	nZ	–	nf_i
	$nZ+1$	nf_i	–
	$nZ-1$	nf_i	–
Outer ring (rotation)	nZ	–	nf_o
	$nZ+1$	nf_o+f_r	–
	$nZ-1$	nf_o-f_r	–
Ball (Z=8)	2n	$2nf_b-f_c$	–
		$2nf_b+f_c$	–
		–	$2nf_b$

Note NRRO changes depending on number of balls, contact angle (radial clearance), material and preload.

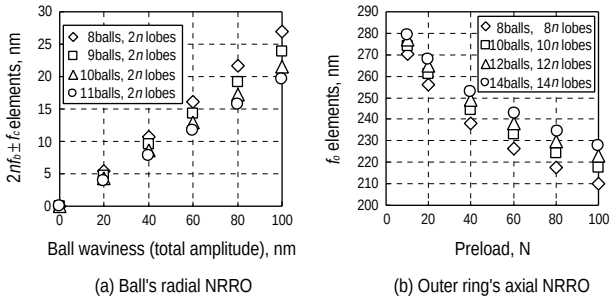

(a) Ball's radial NRRO (b) Outer ring's axial NRRO

Fig. 2 Examples of NRRO analysis

Next, high order elements that have an order higher than the second order are described. Even when a single waviness is taken into consideration, the result of non-linear NRRO analysis shows the occurrence of NRRO element for the number of waviness lobes other than those shown in **Table 2**. To summarize the occurrences, **Table 3** is obtained. That is, the following equation (6) is obtained assuming that the number of waviness lobes of inner and outer rings is W_n and the order is j.

$$W_n = \frac{nZ}{j} \quad \text{Frequency to appear: Inner ring; } nf_i\text{, Outer ring; } nf_o$$

$$W_n = \frac{nZ \pm 1}{j} \quad \text{Frequency to appear: Inner ring; } nf_i\text{, Outer ring; } nf_o \pm 1$$

wherein,
j : Order
W_n : Number of waviness
n : Positive integer
If the right parts of the above equations are a positive number, it indicates the occurrence of NRRO.

..... (6)

If the result of the analysis shows higher order of NRRO, the magnitude of NRRO element is logarithmically reduced accordingly. Thus, it would be normally sufficient to take into consideration up to the second order elements (or up to the third order elements at the maximum). Hereinafter, the second order element of NRRO is discussed.

Table 3 NRRO high order elements (including first-order elements)

Input waviness	Number of waviness lobes	x and y directions [Hz]	z direction [Hz]
Inner ring	$n(Z+1)/j$	nf_i	–
	$n(Z-1)/j$	nf_i	–
	nZ/j	–	nf_i
Outer ring	$n(Z+1)/j$	nf_o+f_r	–
	$n(Z-1)/j$	nf_o-f_r	–
	nZ/j	–	nf_o

n : Positive integer,
j : NRRO order (when the number of waviness lobes is a positive integer)

Figure 3 shows the change of NRRO second order element when the magnitude of raceway waviness, preload, and radial clearance (contact angle) change. **Figure 3** shows the result of performing the input of waviness on its outer ring raceway when j=2 and n=1 in **Table 3**. In **Fig. 3**, the left part shows the magnitude of NRRO second order element of outer ring in the axial direction, and the right part shows that of outer ring in the radial direction.

As can be seen from **Fig. 3**, while the magnitude of NRRO first-order element in the radial direction is constant regardless of preload and the change of radial clearance, the magnitude of the second-order element shows non-linearity. The increase of NRRO second-order element is proportional to the square of the increase of the magnitude of wavinesses. Furthermore, for the input of the same waviness, the second-order element shows different behavior from that of the first-order element; that is, as the number of balls increases, the NRRO second element increases.

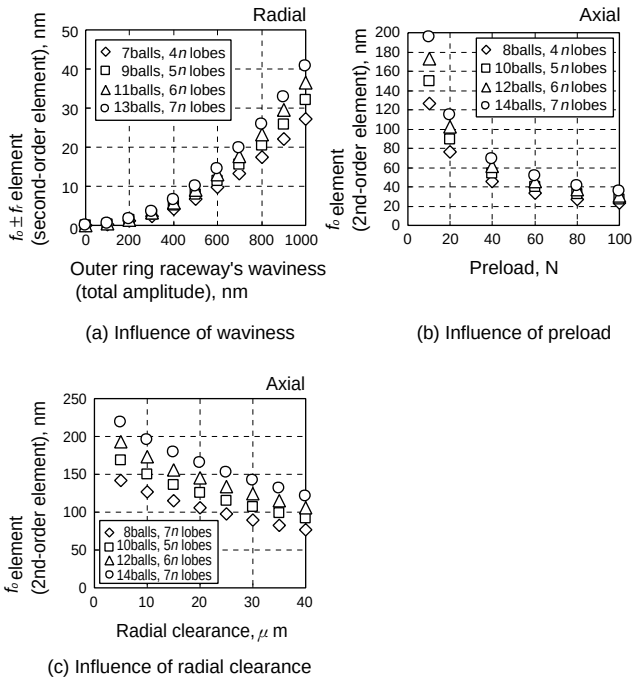

Fig. 3 Analytical result of NRRO second-order elements

Finally, **Fig. 4** shows the NRRO frequency that appears when a single waviness lobe is added to an outer ring raceway. **Figure 4** shows that the number of balls and the number of waviness lobes on an outer ring raceway are 20 and also shows the first-to-third-order NRRO elements. If a single waviness lobe is added to an inner ring (fixed ring), NRRO elements will be generated with the same number of balls and waviness lobes as those for the case of the outer ring and the only difference is the generated frequency, as shown in the above equation (6).

Table 4 NRRO-occurring frequency (1st to 3rd elements)

: 1st element : 2nd element : 3rd element

Number of balls Z	Number of waviness lobes W_n																	
	2	3	4	5	6	7	8	9	10	11	12	13	14	15	16	17	18	19	20
7	fo−	fo−	fo+	2fo+	fo−	fo	fo+	4fo−	3fo−	3fo+	5fo+	2fo−	2fo	2fo+		5fo−	5fo+		
8		fo+	fo	2fo−		fo−	fo	fo+		4fo+	3fo	5fo−		2fo−	2fo	2fo+			5fo
9		fo	fo−	fo+	2fo		fo−	fo	fo+		4fo	3fo−	3fo+	5fo		2fo−	2fo	2fo+	
10		fo−		fo		2fo+		fo−	fo	fo+		4fo−		3fo		5fo+		2fo−	2fo
11			fo+	fo−	fo+	2fo−			fo−	fo	fo+			4fo+	3fo−	3fo+	5fo−		
12			fo		fo		2fo			fo−	fo	fo+			4fo		3fo		5fo
13			fo−		fo−	fo+		2fo+			fo−	fo	fo+			4fo−		3fo−	3fo+
14				fo+		fo		2fo−				fo−	fo	fo+				4fo+	
15				fo		fo−	fo+		2fo				fo−	fo	fo+				4fo
16				fo−			fo			2fo+				fo−	fo	fo+			
17					fo+		fo−	fo+		2fo−					fo−	fo	fo+		
18					fo			fo			2fo					fo−	fo	fo+	
19					fo−			fo−	fo+			2fo+					fo−	fo	fo+
20						fo+			fo			2fo−						fo−	fo

Note) When elements duplicate, lower order element is shown.
nf_o+ : nf_o+f_r, nf_o- : nf_o-f_r

2. 2. 2 NRRO Considering Wavinesses to Inner and Outer Rings

If both of inner and outer rings have wavinesses, NRRO also appears basically as the sum or the difference of single NRRO elements. In this analysis, however, an exceptional NRRO element was found that was generated from the element due to the sum and difference. That is, if the sum or difference of single wavinesses of inner and outer rings is the same as the above-described sum and difference elements, a second-order element will be generated. However, the frequency to appear is different.

Assuming that the numbers of waviness lobes of inner and outer rings are W_{ni} and W_{no}, respectively, NRRO second-order elements are generated in the frequency from the equation (7).

$$
\begin{aligned}
&|W_{ni}+W_{no}| = nZ+1 \\
&\left|\frac{W_{no}(nf_o+f_r)\mp nW_if_i}{W_{ni}\pm W_{no}}\right| = |W_{no}f_r \mp nf_i| \quad [\mathrm{Hz}] \\
&|W_{ni}+W_{no}| = nZ-1 \\
&\left|\frac{W_{no}(nf_o-f_r)\mp nW_if_i}{W_{ni}\pm W_{no}}\right| = |W_{no}f_r \mp nf_i| \quad [\mathrm{Hz}] \\
&|W_{ni}\pm W_{no}| = nZ \\
&\left|\frac{nW_{no}f_o\mp nW_if_i}{W_{ni}\pm W_{no}}\right| = |W_{no}f_r \mp nf_i| \quad [\mathrm{Hz}]
\end{aligned}
\qquad \cdots\cdots (7)
$$

wherein W_{ni}, or $W_{no} \neq nZ$, or $nZ \pm 1$.

3. Result of NRRO's Behavior Analysis

In order to know the essentials of NRRO, it is also important to clarify the behavior of the geometric center of a rotating ring in terms of the bearing characteristics and the measurement method. In this chapter, first, the behavior of a bearing with a single waviness is described. Next, anisotropy of radial NRRO of a stationary inner ring is described.

3. 1 Behavior of Bearing in Which Each Part Has a Single Waviness

To know the behavior of a rotational axis of a bearing in which each part has a single waviness is to provide the basic understanding of NRRO structure. Thus, this behavior is

described below briefly. In this case, the behavior of the geometric center of a rotating axis can be categorized into the following four types of behaviors:

① When a raceway has $nZ \pm 1$ of waviness lobes;
② When a raceway has nZ of waviness lobes;
③ When a ball has $2n$ of waviness lobes; and
④ When balls have differences in diameter or circumferential pitch.

In the case of ②, a bearing performs reciprocating operation at NRRO-occurring frequency in Z direction. In the case of ④, an outer ring moves to a position where force equilibrium occurs and a bearing performs rounding movement in rotational direction at retainer's rotational frequency f_c [Hz]. Thus, the results of the above two cases are omitted. **Figures 4** and **5** show the analysis results of the cases of ① and ③, respectively. When a raceway of a bearing has $nZ \pm 1$ of a single waviness lobe, the bearing performs rounding movement at NRRO-occurring frequency in radial direction (no change in axial direction). However, when rotating with $nZ+1$ waviness, the bearing shows different rounding direction as compared with its direction when rotating with $nZ-1$ waviness. Inner and outer rings of the bearing also show different rotational directions. Since these elements, especially the first-order elements, can be confirmed even by a linear analysis, it is thought that they move with a simple balance of forces. Second-order elements showed similar rounding movement and the diameter of a circle corresponds with the NRRO value and the rotational frequency is the same as NRRO-occurring frequency. The ball behavior shown in **Fig. 5** is a case in which a single ball has two waviness lobes and this is a more complicated behavior compared to those of other elements. **Figure 5** shows the behavior when an outer ring has rotated four times. If the number of rotations to be analyzed is increased, the geometrical center behavior shown in **Fig. 5** will take glass shape. In doing so, the behavior will rotate in the left direction elliptical orbit (1 roundtrip is 1 rotation of a ball) and will gradually shift to the rotational direction, due to the influence of the ball revolution.

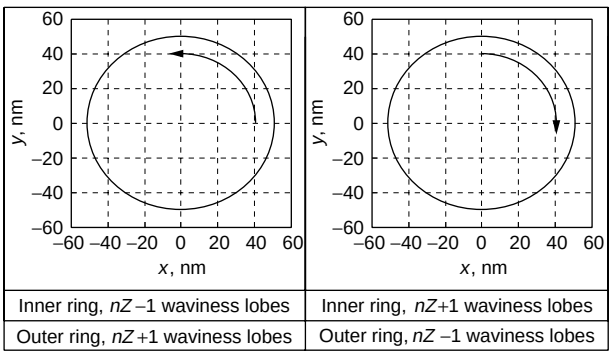

Fig. 4 Behavior of outer ring's geometric center with $nZ \pm 1$ waviness lobes

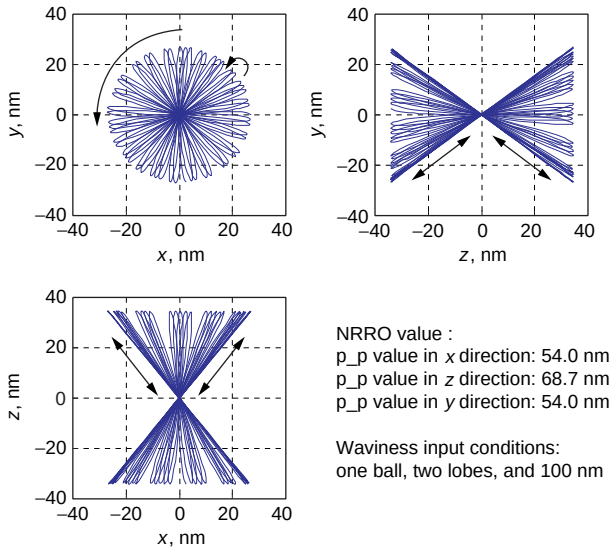

Fig. 5 Outer ring's geometric center behavior with two waviness lobes elements of a ball
(Behaviors with ball rotation axis, contact angle fixed, and four rotations of outer ring)

3. 2 Analysis of Anisotropy When Stationary Ring has $Z \pm 1$ Waviness Lobes Combined

In this section, the behavior when an inner ring has different magnitudes and phases of $Z+1$ waviness lobes and $Z-1$ waviness lobes is described. Analysis examples are shown in **Fig. 6**, where eight balls are used.

From **Fig. 6**, NRRO's Lissajous figure when an inner ring (stationary ring) has $Z+1$ waviness lobes and $Z-1$ waviness lobes, shows linear behavior when the magnitudes of these wavinesses are the same and shows an elliptical configuration when the magnitudes of these wavinesses are different. As can be seen from **Fig. 6**, the major axis shows the sum of the magnitudes of wavinesses and the minor axis shows the absolute value of the difference. The phase difference of inner ring waviness determines the inclination ϕ of the major axis of the ellipse configuration. Assuming that $nZ+1$ waviness lobes have the phase difference of ϕ_{Z+1}, and $nZ-1$ waviness lobes have the phase difference of ϕ_{Z-1}, then the inclination ϕ of the major axis of ellipse orbit of the outer axis geometric center can be calculated by the following equation:

$$\phi = \left\{ \frac{\phi_{nZ+1}(nZ+1) - \phi_{nZ-1}(nZ-1)}{2} \right\} \quad \cdots\cdots (8)$$

Also shown in **Fig. 6** are the inclinations of major axes gained by the above equation (8), shown with parentheses are calculated values. Since f_i element becomes maximum at the sum of $Z \pm 1$ waviness lobe elements (i. e., the major axis of ellipse orbit), anisotropy-considered measurement is necessary.

		Z+1 waviness lobes (9 lobes)			
		amplitude: 0.25, phase: 0°	amplitude: 0.5, phase: 30°	amplitude: 0.75, phase: 60°	amplitude: 1, phase: 90°
Z–1 waviness lobes (7 lobes)	Amplitude: 0.25, Phase:0°	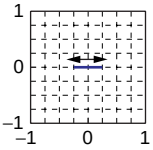	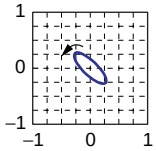	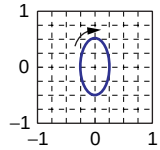	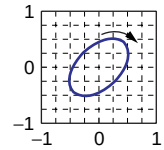
		a=0.5, b=0	a=0.75, b=0.25	a=1, b=0.5	a=1.25, b=0.75
		ϕ =0°	ϕ =135°	ϕ =90°(270°)	ϕ =45°(405°)
	Amplitude: 0.5, Phase:30°	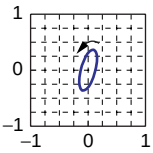	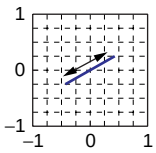	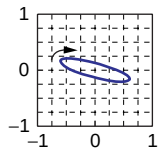	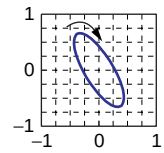
		a=0.75, b=0.25	a=1, b=0	a=1.25, b=0.25	a=1.5, b=0.5
		ϕ =75°(–105°)	ϕ =30°	ϕ =165°	ϕ =120°(300°)
	Amplitude: 1, Phase:90°	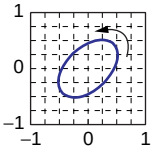	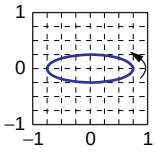	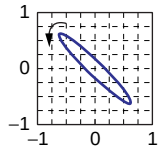	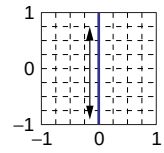
		a=1.25, b=0.75	a=1.5, b=0.5	a=1.75, b=0.25	a=2, b=0
		ϕ =45°(–315°)	ϕ =0°(–180°)	ϕ =135°(–45°)	ϕ =90°

Fig. 6 Analysis example of anisotropy with combination of Z±1 waviness lobes on inner ring
(Z=8, a: length of major axis, b: length of minor axis, ϕ : inclination of major axis)

3. 3 Behavior When a Plurality of Wavinesses Exist

In this section, the behavior when raceways have all first-order elements (n=1) is described.

Figure 7 shows the analysis result thereof. In this case, eight balls are used and inner and outer rings have seven, eight, and nine waviness lobes, each of which has a length of 20 nm. That is, a total of six elements are added to the inner and outer rings. **Figure 7** shows the result of plotting the data in which these rings are rotated with a speed of 5 400 min^{-1} for 0.8 second, totaling the 4 096 data. As can be seen in **Fig. 7**, even all first-order elements (n=1) existing in races show extremely complicated behavior configurations. Checking the movement of outer ring's geometric center also showed a complicated behavior in which all coordinate planes include runouts in the front and rear directions. ADORE analysis also provided the behavior having approximately the same configuration, thereby verifying that the absolute value error between this program and ADORE is maximum 1.5%. Calculation time needed by this model was about five seconds using a Pentium Ⅲ(850 MHz) computer.

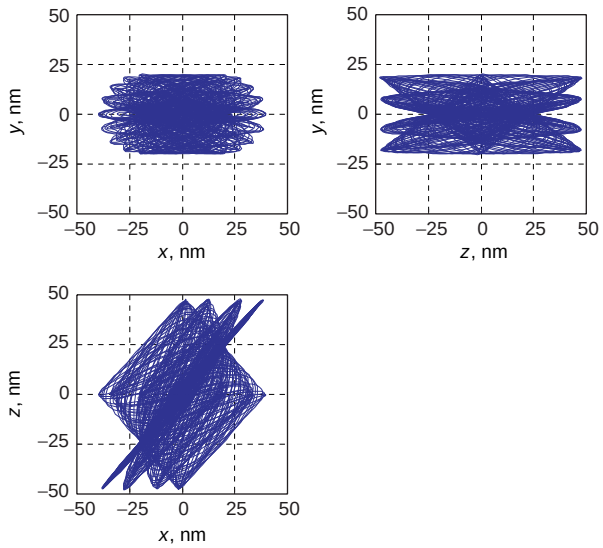

Fig. 7 Behaviors with a plurality of wavinesses (Z–1, Z and Z+1 waviness lobes (20 nm) are added to inner and outer rings)

4. Features of 3-dimensional NRRO Analysis Program

The 3-dimensional NRRO analysis program developed can provide the time-lapse-concept-incorporated analysis of inner and outer rings' wavinesses, ball waviness, and ball pitch error of a ball bearing, covering almost all kinds of NRRO analyses. This 3-dimensional NRRO analysis program also can provide animated behaviors of outer ring's geometric center and each bearing part to allow users to visually confirm the behavior, providing many findings.

Although the details are omitted due to space limitations, the analysis result gained by this 3-dimensional NRRO analysis program showed good correspondence with that by ADORE, proving the validity thereof[12].

As can be seen from the above example of how big influence of NRRO has on HDD, reduction of NRRO is the key to improve the recording density of HDD[13, 14].

In such a situation, NRRO analysis by this program will provide a lot of insights for R&D efforts for the NRRO reduction. This program can provide sufficient analysis capacity for the 3-dimensional NRRO analysis that takes into consideration the bearing rolling contact surface's wavinesses, providing the data regarding the basic characteristics of NRRO.

5. Conclusions

Shown below are the results gained from the development of the semi-dynamic 3-dimensional NRRO analysis program for HDD ball bearings to analyze non-linear characteristics and behaviors of NRRO.

1) NRRO's first-order elements in the radial direction caused by inner and outer rings' $nZ \pm 1$ waviness lobes equal to total amplitude of waviness and have a proportional relationship with the magnitude of waviness, regardless of material, preload, contact angle, and the number of balls.
2) NRRO caused by nZ waviness lobes in the inner and outer rings' axial direction and NRRO caused by $2n$ ball waviness lobes showed non-linearity.
3) All of NRRO high order elements caused by inner and outer rings' waviness showed non-linearity. The number of high order elements generated by a single waviness could be formulated.
4) The relationship was clarified between the number of waviness lobes and a second-order element-occurring frequency when inner and outer rings respectively have a single waviness.
5) It was clarified that when a stationary ring having layered structure of $Z+1$ waviness lobes and $Z-1$ waviness lobes, outer ring's geometric center has an ellipse configuration and the inclination of the major axis of the ellipse configuration was formulated.

It is considered that this 3-dimensional NRRO analysis program will further be able to analyze the influence of ball waviness by fixing a ball's rotation axis and contact angle and, if behavior analysis techniques are further developed, it has further possibility to provide new findings for ball bearings' behavior.

References

1) O. Gustafsson: SKF Report, AL 61 L 032 (1961)
2) O. Gustafsson: SKF Report, AL 62 L 005 (1962)
3) T. Igarashi: "Korogari Jikuuke no onkyou oyobi shindou ni kansuru kenkyuu ronbunshuu" Igarashi Lab. in Department of Mechanical Eng., Nagaoka University of Technology (1986).
4) G. Bonchard and L. Lau: "An Investigation of Non-repeatable Spindle Runout" IEEE Transactions on Magnetics, **23**, 5 (1987) 3687.
5) W. O. Richter and F. E. Talke: "Nonrepeatable Radial and Axial Runout of 5 1/4" Disk Drive Spindles" IEEE Transactions on Magnetics, **24**, 6 (1988) 2760.
6) K. Ono, et al.: "Analysis of Nonrepeatable Radial Vibration of Magnetic Disk Spindles", Transaction of the ASME, 113 (1991-7) 292.
7) T. Sakaguchi and Y. Akamatu: NTN Technical Review, 69 (2001) 69.
8) S. Noguchi and K. Ono: Transactions of the JSME, **64**, 620, C (1998-4) 282.
9) S. Deeyiengyang and K. Ono: Transactions of the JSME, **66**, 648, C (2000-8) 32.
10) P. K. Gupta: "Advanced Dynamics of Rolling Elements", Springer-Verlag (1984).
11) T. A. Harris: "ROLLING BEARING ANALYSIS-Third Edition", JOHN WILEY & SONS, INC. (1991).
12) S. Tada: Koyo Engineering Journal, 160E (2002) 29.
13) H. Takii: Journal of the JSPE, **67**, 7 (2001) 1083.
14) M. Musaka: Koyo Engineering Journal, 160E (2002) 15.

S. TADA*

* *Bearing Research & Development Department, Research & Development Center, Dr.*